Advanced Composite Materials
Publication details, including instructions for authors and subscription information:
http://www.tandfonline.com/loi/tacm20

Studies on microyield behavior of SiCp/2024Al composite materials

Fan Zhang , Xiaocui Li & Cheng Jin

Version of record first published: 02 Apr 2012.

To cite this article: Fan Zhang , Xiaocui Li & Cheng Jin (2000): Studies on microyield behavior of SiCp/2024Al composite materials, Advanced Composite Materials, 9:1, 11-23

To link to this article: http://dx.doi.org/10.1163/156855100300132938

Adv. Composite Mater., Vol. 9, No. 1, pp. 11–23 (2000)

Studies on microyield behavior of SiCp/2024Al composite materials

FAN ZHANG *, XIAOCUI LI and CHENG JIN

State Key Laboratory of Metal Matrix Composites, Shanghai Jiao Tong University, Shanghai 200030, P. R. China

Received 19 January 1998; accepted 31 December 1998

Abstract—Microyield behavior of silicon carbide particles reinforced 2024 aluminum alloy (SiCp/2024Al composites) with three volume fractions of SiCp were investigated in this paper. The results of the studies showed that the composites exhibited some types of notable strain relaxation before microyielding when subjected to an applied stress far lower than conventional yielding stress. The microyield mechanism did not conform to the classical linear relation between the applied stress (σ) and square root of plastic strain ($\varepsilon_p^{1/2}$), proposed by Brown and Lukens. Microyield strength could be strongly affected by heat treatment routes. The thermal processing with large temperature change, such as high temperature quenching or annealing, rapid cooling to liquid nitrogen temperature, thermal cycling with large upper-lower cyclic temperature interval, etc., would lead to deterioration of microyield strength, whereas an appropriate aging treatment would significantly increase microyield strength of the SiCp/2024Al composites. TEM and X-ray diffraction analyses revealed the relationship between microyield behavior and microstructures. In general, dispersed strengthening phase S′, lower residual stresses and lower population of movable dislocations would be beneficial to microyield strength of the SiCp/2024Al composite materials. The effect of SiCp on microyield strength was dependent to thermal processing history.

Keywords: Microyield behavior; strain relaxation; SiCp/2024Al composite; heat treatment; ΔCTE stress.

1. INTRODUCTION

Because they possess a wide range of superior properties, such as high specific strength and Young's modulus, lower thermal conductivity and thermal expansion coefficients, aluminum alloy composite materials reinforced with silicon carbide particles (SiCp/Al) are being gradually employed in some optical precision instruments and systems [1]. As they are used for precision devices, dimensional stability

*To whom correspondence should be addressed. Institute of Composite Materials, Shanghai Jiao Tong University, 1954 Hua Shan Road, Shanghai 200030, P. R. China.

of the material is very important. The most common causes of dimensional instability in materials usually are phase transformation, relief of residual stresses, and microplastic deformation resulting from an applied stress. The effects related to phase transformation and residual stresses can generally be controlled by properly selecting component materials and appropriate dimensional stabilizing heat treatment procedures. However, the dimensional instability induced by microplastic deformation is very difficult to control because the internal stresses, which may come from assembly operation, shocking or vibrating in service, are unavoidable. So it is desirable to improve the resistance to microplastic deformation (i.e. microyielding) of materials, and the microyield strength (MYS — the applied stress at plastic strain $\varepsilon_p = 10^{-6}$) is recommended as one important measurement of dimensional stability [2, 3].

Little attention had been paid to microplasticity of metallic materials before the 1960s. The early achievements have been gathered into some collected works and treatises [3–5]. Also, since SiCp/Al composite is a new kind of material which is still being developed, the testing of microplasticity is quite difficult; only a few reports have appeared so far concerning microyield behavior of the composites [6–9], resulting in a lack of understanding about microyield behavior, especially the effects of heat treatments on the microyield strength of SiCp/Al composite materials. We have selected a most promising system — SiCp/2024Al — as the object of our investigations; the present paper deals with the microyield behavior and the effects of different heat treatments in order to get basic knowledge about the rule, mechanism and factors that influence microyielding in this composite material.

2. EXPERIMENTAL

2.1. Materials

A commercial 2024 aluminum alloy (Al–4.00%Cu–1.31%Mg–0.58%Mn) was selected as the matrix of our experimental composites, and silicon carbide particles (nominal diameter, 7μm) were used as the reinforcement. By a vacuum pressure infiltration method, which consists of two major steps — preparation of preform and infiltration of preform — the 35%, 45% and 55%SiCp/2024Al composite materials were fabricated (further details of the method may be found in an earlier paper, ref. [10]). Then dog bone-shaped coupons of 3 mm thickness, 6 mm width and 8 mm gage length were made by means of electric charge machining.

2.2. Heat treatment

The heat treatments in this work were divided into three stages for different aims

(1) To check the effects of different types of heat treatment on microyield behavior, several different procedures were employed with 35%SiCp/2024Al, in addition to the as-fabricated specvimen; these are listed in Table 1.

Table 1.
Different types of heat treatment routes for 35%SiCp/2024Al

Regime	Description
Casting	As fabricated by vacuum pressure infiltration
Annealing	400 °C × 3 h, furnace cooling
Quenching	500 °C × 1 h, water quenching
Rapid cooling	500 °C × 1 h, water quenching +190 °C × 24 h, air cooling to room temperature + quenching into liquid nitrogen (−196 °C) and keeping for 1h, then lying in air to room temperature
Natural aging	500 °C × 1 h, water quenching + keeping at room temperature for more than 48 h
T6	500 °C × 1 h, water quenching + 190 °C × 8 h, air cooling
Quenching + Cycling	500 °C × 1 h, water quenching + (190 °C × 2.5 h ⇔ −196 °C × 1 h, 3 times)
Annealing + Cycling	400 °C × 3 h, furnace cooling + (190 °C × 2.5 h ⇔ −196 °C × 1 h, 3 times)

Table 2.
Regime parameters of aging and thermal cycling treatments for 35%SiCp/2024Al

Regime	Description
Aging	(1) 500 °C × 1 h, water quenching + 190 °C ×(4, 8, 12, 16, 20 h) respectively, air cooling (2) 500 °C ×1 h, water quenching + (110 °C, 150 °C, 190 °C, 230 °C, 270 °C) × 8 h respectively, air cooling
Cycling	(1) 500 °C × 1 h, water quenching + (190 °C × 2.5 h ⇔ −196 °C × 1 h for 1, 3, 5 times respectively) (2) 500 °C × 1 h, water quenching + (110 °C, 150 °C, 190 °C, 230 °C, 270 °C) × 2.5 h ⇔ −196 °C × 1 h, 3 times
T6 + Cycling	500 °C ×1 h, water quenching + 190 °C × 8 h, air cooling, + (190 °C × 2.5 h ⇔ −196 °C × 1 h, 3 times)

(2) To examine the effects of regime parameters of aging and thermal cycling which are traditional dimensional stabilizing heat treatments for aluminum alloys on microyield behavior, the treating routes listed in Table 2 were carried out for 35%SiCp/Al.

(3) In order to understand the effects of SiCp volume fraction on microyield behavior, three volume fraction composites were heat treated by the treating routes listed in Table 3.

2.3. Testing of microyield behavior

After the above thermal treatments, the specimens were tested on a MTS New 810 tester by a continuous loading method [11]. In contrast to the step load–

Table 3.
Heat-treatment regimes for 35%, 45%, 55%SiCp/2024Al

Regime	Description
Aging	500°C × 1h, water quenching + 190°C × 24h, air cooling
Thermal Cycling	500°C × 1 h, water quenching + (190°C × 2.5 h ⇔ −196°C × 1 h for 3 times)

unload method, the former could diminish the side effect of micromechanical cyclic strengthening. But the errors of strain measurements in the continuous loading method were slightly higher than those in the load–unload method because the Young's modulus, to evaluate plastic strain, is quite difficult to determine rigorously.

The load train design of the MTS New 810 machine permitted an acceptable level of alignment. The continuous tension was performed with a load control mode at a rate of 3 kN/min. The strain was measured using the MTS special extensometer which has a sensitivity of 6×10^{-7} and 0.006 maximum range. The acquisition of applied stress (σ) and strain (ε) data, as well as determination of Young's modulus (E) were carried out using the MTS system microcomputer with special testing software. The plastic strain (ε_p) was calculated according to the equation: $\varepsilon_p = \varepsilon - \sigma/E$. Finally, the $\sigma \sim \varepsilon_p$, $\sigma \sim \varepsilon_p^{1/2}$ relationships and microyield strength (MYS — the stress at $\varepsilon_p = 10^{-6}$) could be obtained.

To check the relationship between microyield behavior and microstructure, a JEOL 200CX electron microscope was used to perform TEM analyses, and X-ray diffraction analyses were performed with a D/Max-II A diffractometer. In X-ray tests, the (222) diffraction peak of the 2024 aluminum matrix was selected to qualitatively analyze microscopic residual stresses in the matrix of the composites.

3. RESULTS AND DISCUSSIONS

3.1. Microyield behavior

The experimental σ *versus* ε_p curves for several typical treated specimens are shown in Fig. 1. It is noted that there exists quite apparent small permanent strain at very low applied stress. The strain observed in our experimental work seems to be of a variety of different types, which are schematically illustrated in Fig. 2 and they bear no clear relation to corresponding heat treatment routes. But they can be generally divided into 'positive', 'negative' and 'mixed' strain respectively. For convenience sake, we define them as 'strain relaxation' in the present paper. It has been found that some traditional metallic materials, such as copper [12], aluminum alloys [13], invar alloys [14] and titanium alloys [15], could present either a positive or negative relaxation during the period of microstrain. However, there are no corresponding reports on metal matrix composites, so thus far the nature of the strain relaxation still remains unknown. Reichenbach *et al*. [16] proposed that the negative strain has

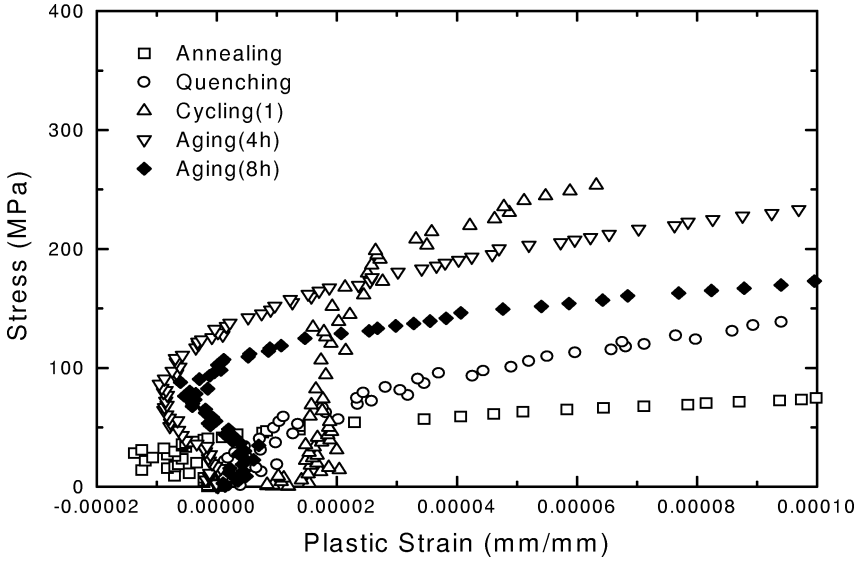

Figure 1. Experimental σ *versus* ε_p curves of 35%SiCp/2024Al composite under several typical treatments (see Table 2).

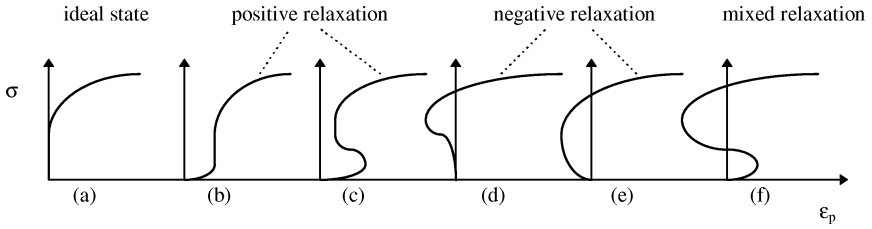

Figure 2. Schematic illustration of several kinds of permanent strain at near zero applied stress.

been attributed variously to creep of the gage-bonding agent, improper bonding of the strain gages, or exceeding the elastic strain capability of the cement. Hordon *et al*. [13] stated that the negative strain was the outcome of the 'surface effect'. Though these may provide explanations in some instances, there are others where these explanations do not appear to suffice. In our work, the negative strain was also obtained by the continuously loading method, suggesting that the negative residual strain reflects a real behavior of the specimens rather than that of the strain gages. In addition, an anelasticity effect produced by jumping of solution atoms or impurity atoms in materials may be one reason for the positive relaxation, but under no circumstances does it cause the negative relaxation.

So it is rationally believed that the strain relaxation has a bearing on the rearrangement of some microstructures in materials. For the SiCp/2024Al composite materials, due to a large difference in the thermal expansion coefficients between the SiC particles and the aluminum matrix, the microstructure of the composites after high temperature fabrication always present the following features [17–22]:

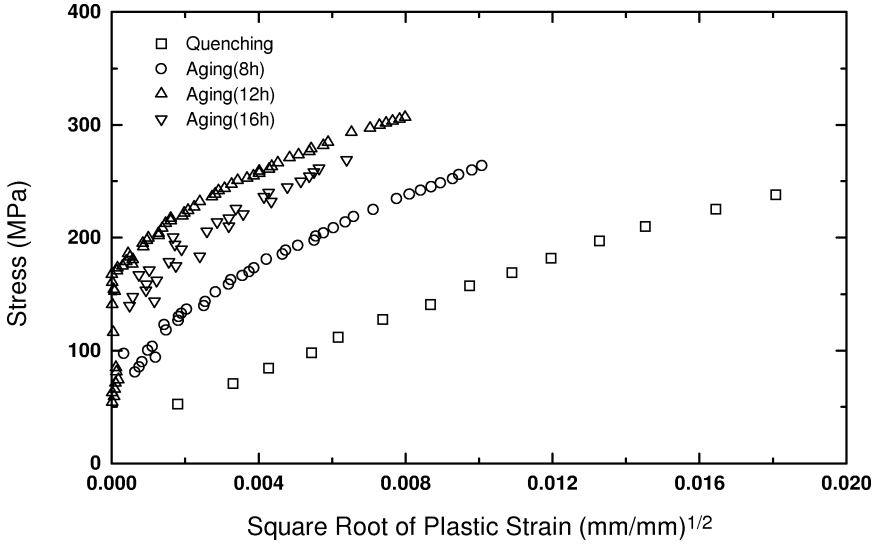

Figure 3. Experimental σ *versus* $\varepsilon_{\mathrm{p}}^{1/2}$ curves of 35% SiCp/2024AL composite under several heat treatments (see Table 2).

– large residual thermal mismatch stress imparted by various processing operations;

– high population of mobile dislocations induced by the relaxation of ΔCTE stresses;

– high local stress concentration introduced by irregularly shaped SiC platelets.

Thus, even subjected to a very low applied stress, the local stress at some microzone in the matrix could exceed the conventional yield stress. Owing to the complexity of stress concentration and ΔCTE stress distribution, the direction of local stress may not be along that of the applied stress and the strain relaxation can take place in all possible orientations. Only when the applied stress reaches a higher amplitude level will the strain led by dislocation motion proceed in the expected direction and exhibit a 'whole' microyielding characteristic. The microyield behavior discussed below in the paper is that which arises when the strain relaxation before microyielding has been removed.

Figure 3 demonstrates a group of experimental σ *versus* $\varepsilon_{\mathrm{p}}^{1/2}$ curves under some aging treatment conditions. In this figure, the data of the elastic stage and the data of $\varepsilon_{\mathrm{p}} > 10^{-4}$ (the range of $\varepsilon_{\mathrm{p}} > 10^{-4}$belongs to the macroyield stage) have been removed in order to focus on the 'whole' microyield behavior. It can be seen that the relationship between applied stress (σ) and square root of plastic strain ($\varepsilon_{\mathrm{p}}^{1/2}$) present a curved line form and does not obey the Brown–Lukens equation [23]:

$$\sigma = \sigma_0 + K\varepsilon_{\mathrm{p}}^{1/2},$$

where σ_0 is the initial resistance to dislocation gliding, K is a coefficient associated with the shear modulus, G, and is given by

$$K = \sqrt{\frac{2G\sigma_0}{\rho \times d}},$$

where d is the mean grain size, and ρ is the dislocation density.

The Brown–Lukens relationship was derived through the hypothesis that the dislocation sources are uniformly distributed in the whole volume of material's interior and only a grain boundary can hinder dislocation movement, so it is valid only for a single crystal or for polycrystalline metals in principle. In the case of our experimental materials, there are two microstructure factors that deviate from the above basic assumptions: first, in addition to the grain boundary there exists another strong barrier to dislocation, namely, the SiCp particles; secondly, distribution of dislocations in the matrix is not uniform. Some authors have reported that, due to relief of ΔCTE stress, the dislocation density near the SiCp-matrix interface is much higher than that in the interior of the matrix [24, 25]. Based on the experimental data (see Fig. 3) which revealed the higher work hardening rate at the very beginning of microplastic deformation than that at the later stages, it is probable that initial microyielding of the composite is the result of movement of those dislocations which are located near SiC particles in the matrix.

3.2. Effects of different types of heat treatments on microyield strength

Microyield strength (MYS) reflects the initial resistance to microplastic deformation and is an important measure of microyield behavior and dimensional stability under short-term loading conditions. Figure 4 illustrates the microyield strength of differently treated specimens of 35%SiCp/2024Al.

Obvious differences in MYS can be seen for these different heat treatments. The conditions having age hardening effects, such as natural aging, T6 and quenching + cycling, exhibited high MYS whereas the other treatments, such as casting, annealing, rapid cooling, and annealing + cycling, were of MYS lower than 50 MPa. The reason why aging treatment enhances MYS is related to participation of the strengthening phase S′ ($Al_{12}Mg_2Cu$) in the matrix.

Figures 5a and b show TEM micrographs of T6 treated and quenching + thermal cycled specimens respectively. For both these treatments, the hard strengthening phase S′ participated dispersed in the matrix. It has very small size (about 50 nm) and interspacing (about 50 $\sim$ 100 nm), but could thus provide a strong obstacle to short distance gliding of dislocation. It is noted from Fig. 4 that T6 followed by rapid cooling treatment lowered MYS values from 143 to 27 MPa. This dramatic drop of MYS is associated with largely increasing residual stresses in the material. As mentioned above, owing to near one order of difference in coefficients of thermal expansion between SiC particles and the matrix, it is natural to produce ΔCTE

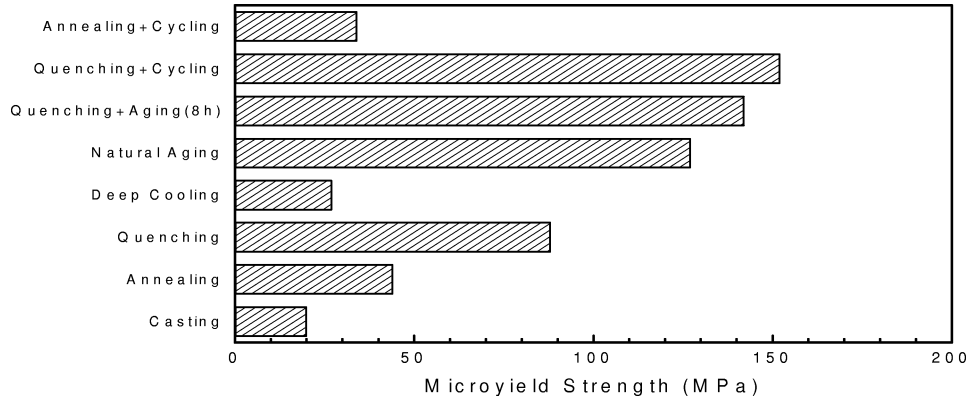

Figure 4. Experimental MYS for different heat treatment conditions (see Table 1).

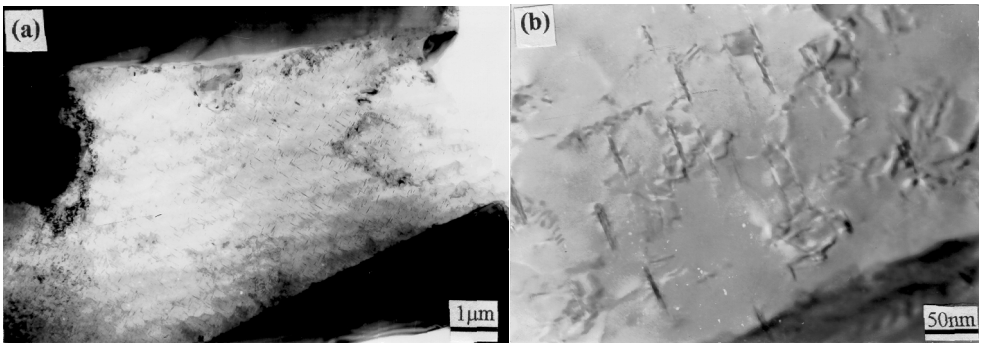

Figure 5. TEM images of T6 treated (a) and quenching + 3 times' cycled (b) specimens.

stress when the temperature changes. The larger the change of temperature (ΔT), the larger is the ΔCTE stress. Some experimental results and theoretical analysis has revealed [26–28] that even if ΔT is quite small, the local ΔCTE stress near the SiCp/matrix interfaces would exceed the yield stress of the matrix, leading to the stress relief and simultaneously producing a large population of dislocations. This state of high residual stress and high dislocation density is significantly harmful to the MYS of the materials. It should be noted also that, due to intrinsic ΔCTE stress of the material, the thermal cycling would not be favored in MYS, as has been shown by annealing (MYS = 44 MPa) and annealing followed by thermal cycling 5 times (MYS = 34 MPa). However, in comparison to quenching, subsequent thermal cycling raised the MYS from 88 to 152MPa, suggesting that age hardening plays an important role in MYS (see Fig. 5b). It is expected that if the number of cycles were increased, which implies that the aging effects would gradually disappear due to an 'overaging' mechanism, then the MYS would be lowered.

Based on the above experimental results, the quenching followed by aging or thermal cycling could be considered as two appropriate treatments beneficial to

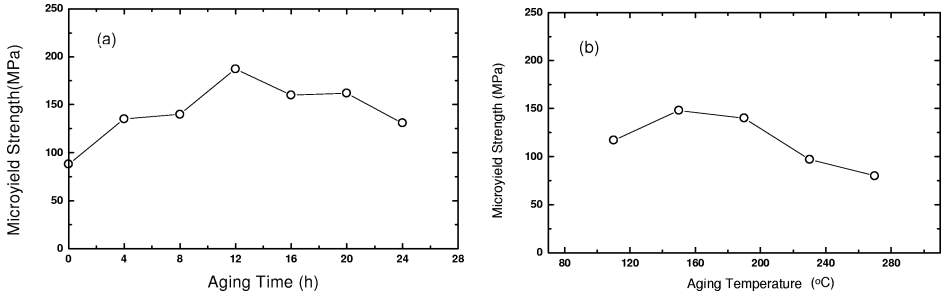

Figure 6. The effects of aging time (a) and aging temperature (b) on MYS (treatments see Table 2).

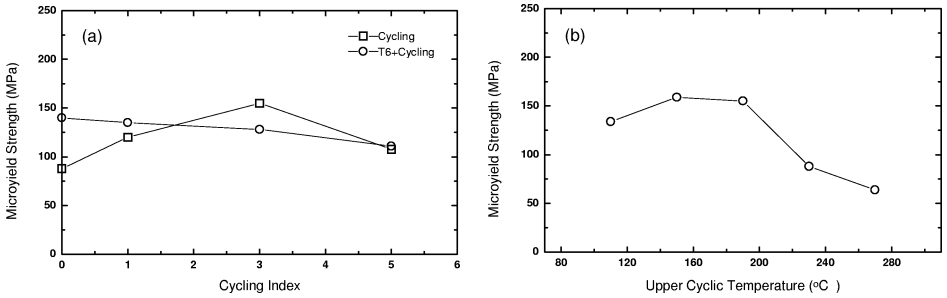

Figure 7. The effects of thermal cycling number (a) and upper cyclic temperature (b) on MYS (treatments see Table 2).

MYS of the composite. In order to further understand the variations in MYS under various aging and cycling conditions, the effects of parameters for the two treatments on MYS have been studied in detail. The results are demonstrated in Figs 6 and 7, respectively.

It can be seen from Fig. 6 that, no matter what aging time or aging temperature was employed, MYS presents a peak value. In other words, there exists an optimum time or temperature at which MYS reaches its maximum value. The condition associated with the optimal parameter corresponds to 'peak aging'. The 'under-aging' or 'overaging' that corresponds to shorter or longer time, and lower or higher temperature, respectively, would be disadvantageous to MYS of the material. This rule is the same as that found in traditional aluminum alloys and implies again that MYS of the composite, like macroyield strength, is also controlled by participation in some way of the second strengthening phase (S′). For quenching followed by thermal cycling also we can find the 'peak values' phenomenon in MYS *versus* cycling index or upper cyclic temperature relationships (see Fig. 7). These indicate the comprehensive influence of aging hardening, increasing both ΔCTE stress and dislocation density. At an early stage of treatment, which means a lower cycling number or smaller cyclic temperature interval, aging strengthening takes the leading role, while at the later stages, the effects of aging have been diminished due to 'overaging' and MYS is strongly affected by residual stresses and mobile dislocation density.

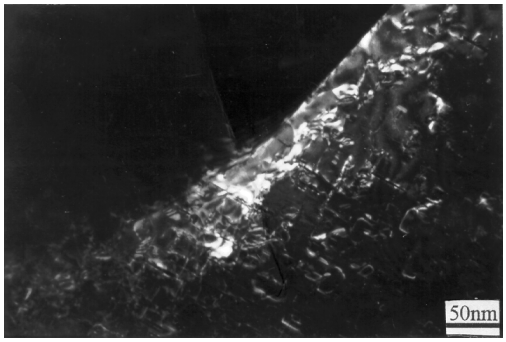

Figure 8. TEM dark image of 5 times cycled specimen.

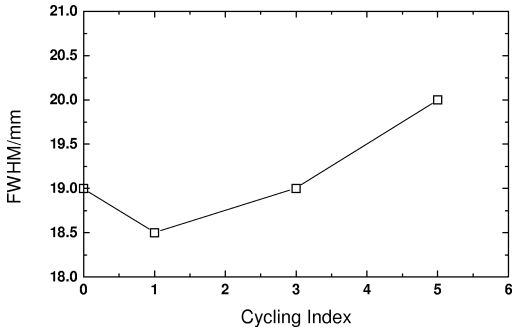

Figure 9. Relationship between FWHM of $(222)_{Al}$ peak and cyclic numbers.

Figure 8 shows a TEM micrograph of a 5 times' cycled specimen. A large number of dislocations generated by ΔCTE stress during cycling process, which has high mobility, were observed near the interface. In addition, the increase in the half-width of the $(222)_{Al}$ peak with cycling index indicated the rising of microscope residual stress (see Fig. 9). The two microstructure changes resulted in the decreasing of MYS. So it can be proposed that without an age hardening effect, the thermal cycling treatment is harmful to MYS of SiCp/2024Al composite materials. This deduction had been verified from the experimental data in comparison between annealing and annealing followed by thermal cycling (see Fig. 4), as well as cycling and T6 followed by cycling (see Fig. 7a).

3.3. Effects of SiCp volume fraction on MYS

The incorporation of SiC particles in aluminum matrices will generate some new characteristics different from those of matrix alloys. The main properties of interest to us here are: (1) a new kind of obstacle to dislocation; (2) lower stresses in the matrix than conventional mean stresses when subjected to a load; (3) high degree of stress concentration from irregularly shaped SiC particles; (4) high level of residual

Table 4.
Effects of SiCp volume fraction on microyield strength of SiCp/2024Al composites

Heat treatments	Microyield strength (MPa)		
(see Table 3)	35%SiCp	45% SiCp	55% SiCp
Aging	131	103	160
Thermal cycling	155	138	104

ΔCTE stresses, and (5) high density of dislocations. The first two factors are favorable to MYS, but the last three factors are just the opposite. Therefore, it is anticipated that the effects of SiCp on MYS are dependent on heat treatment routes.

Table 4 gives MYS values of 35%, 45%, and 55%SiCp/2024Al composites under aging for 24 h (overaging) and thermal cycling 5 times (analogous to overaging) conditions respectively. After 24 h aging, the aging hardening effect has vanished and the action of SiCp pinning dislocation becomes highly evident; thus, the increasing of SiCp volume fraction could raise MYS of the material. But for cycling treatment, the increase in SiCp volume fraction would aggravate the ΔCTE stress level, raise dislocation density, and finally lead to decreasing of MYS. So it can be considered that the addition of SiCp is harmful to the MYS of composite materials under those heat treatment conditions which involve a large change in temperature.

4. CONCLUSIONS

(1) The strain relaxation prior to microyielding is quite obvious in SiCp/2024Al composite materials, and is believed to be associated with the intrinsic ΔCTE stress and high population of mobile dislocations in the matrix.

(2) The relationship between the applied stress (σ) and square root of plastic strain ($\varepsilon_p^{1/2}$) does not obey the Brown–Lukens equation: $\sigma = \sigma_0 + K\varepsilon_p^{1/2}$, which indicates that the microyield mechanism of the composites is not same as that of traditional aluminum alloys.

(3) Dispersed participation of the second strengthening phase S′ could significantly improve MYS of the composite materials.

(4) Thermal cycling treatment is not beneficial to MYS except for quenching followed by 3 times cycling which is at the ‘peak aging’ stage.

(5) The effects of SiCp on MYS are dependent on the heat treatment routes. In general, for those treatments having a large temperate change, the increase of SiCp volume fraction is harmful to MYS.

REFERENCES

1. W. R. Mohn and D. Vukobratovic, Engineered metal matrix composites for precision optical systems, *SAMPE Journal* (1/2), 26–35 (1988).
2. J. Wittenauer, D. L. Yaney and R. E. Lewis, Microyielding in Fe-36Ni: Role of carbon and thermal processing, *Scripta. Metallurgica et Materialia* **31** (11), 1531–1536 (1994).
3. M. L. Khenkin and E. Kh. Lokshin, *The Dimensional Stability of Metals and Alloys in Precision Machine and Instrument Manufacturing*. Science Press, Beijing (1981) (Chinese translation).
4. C. J. McMahan, Jr., *Microplasticity*. Interscience Publishers, New York, NY (1968).
5. C. W. Marschall and R. E. Maringer, *Dimensional Instability — An Introduction*, 1st edn.. Pergamon Press, Oxford (1977).
6. P. J. Withers *et al*., Comments on "The strength differential and Bauschinger effects in SiC-Al composites", *Mater. Sci. and Eng. A* **A108**, 281–284 (1989).
7. Y. C. Li and X. Y. An, Effects of dimensional stabilizing heat treatments on the dimensional stability of SiCp/Al composites, *The Chinese Journal of Nonferrous Metals* **2** (3), 76–80 (1992).
8. R. Hamann, P. F. Gobin and R. Fougeres, A study of the microplasticity of some discontinuously reinforced metal matrix composites, *Scripta Metallurgica et Materiatia* **24**, 1789–1794 (1990).
9. Z. L. Li and Z. K. Yao, Studies on dimensional stabilizing heat treatments of SiC_w/Al composites, *Ordnance Material Science and Engineering* **11**, 1–5 (1991) (in P. R. China).
10. X. Li, F. Zhang, C. Jin and F. Zhong, Study on the microstructures and mechanical properties of low particle volume fraction SiCp/LY12 produced by vacuum pressure infiltration casting techniques, *Materials for Mechanical Engineering* **22** (1), 26–29 (1997) (in P. R. China).
11. R. D. Carnahann, R. J. Arsenault and G. A. Stone, Effects of purity and temperature on dynamic microstrain of Niobium (Columbium), *Trans. of the Met. Soci. of AIME* **239** (8), 1193–1199 (1967).
12. D. A. Thomas and B. L. Averbach, The early stages of plastic deformation in copper, *Acta Met.* **7**, 69–75 (1959).
13. M. J. Hordon, B. S. Lement and B. L. Averbach, Influence of plastic deformation on expansivity and elastic modulus of aluminum, *Acta Met.* **6**, 446–453 (1958).
14. G. W. Geil and I. J. Feinberg, Microplasticity II Microstrain behavior of normalized 4340 steel and annealed Invar. US National Bureau of Standards Report No. 9996 (1969).
15. C. W. Marschall, R. E. Maringer and F. J. Cepllina, Dimensional stability and micromechanical properties of materials for use in an orbiting astronomical observatory, *AIAA* Paper No. 72–325 (1972).
16. G. S. Reichenbach, D. A. Brown and P. G. Russell, Yield behavior of certain alloy steels at low strain values, *Trans. ASM* **54**, 413–429 (1961).
17. M. Vogelsang, R. J. Arsenault and R. M. Fisher, An *in-situ* HVEM study of dislocation generation at Al/SiC interfaces in metal matrix composites, *Met. Trans.* **17A**, 379–389 (1986).
18. R. J. Arsenault and R. M. Fisher, Microstructure of fiber and particulate SiC in 6061 Al composites, *Scripta Met.* **17**, 67–71 (1983).
19. J. K. Lee, Y. Y. Earmme, H. I. Aaronson and K. C. Russell, Plastic relaxation of the transformation strain energy of a misfitting spherical precipitate: Ideal plastic behavior, *Met. Trans.* **11A**, 1837–1847 (1980).
20. W. S. Miller and F. J. Humphreys, Strengthening mechanisme in particulate metal matrix composites, *Scripta Metallurgica et Materialia* **25**, 33–38 (1991).
21. V. C. Nardone and X. M. Prewo, On the strength of discontinuous silicon carbide reinforced aluminum composites, *Scripta Met.* **20**, 43–48 (1986).
22. Y. Flom and R. J. Arsenault, Deformation in Al-SiC composites due to thermal stresses, *Mater. Sci. Engng.* **75**, 151–167 (1985).
23. N. Brown and K. F. Lukens, Microstrain in polycrystalline metals, *Acta Met.* **9**, 106 (1961).

24. M. Tara and T. Mori, Dislocations punched-out around a short fiber in a short fiber metal matrix composite subjected to uniform temperature change, *Acta Metall.* **35**, 155–162 (1987).
25. R. J. Arsenault and N. Shi, Dislocation generation due to differences between the coefficients of thermal expansion, *Mater. Sci. Engng.* **81**, 175–187 (1986).
26. R. J. Arsenault, L. Wang and C. R. Feng, Strengthening of composites due to microstructural changes In the matrix, *Acta Metall. Mater.* **39** (1), 47–57 (1991).
27. N. Shi, B. Wliner and R. J. Arsenault, An FEM of the plastic deformation process of whisker reinforced SiC/Al composites, *Acta Metall. Mater.* **40** (11), 2841–2854 (1992).
28. R. J. Arsennault and M. Taya, Thermal residual stress in metal matrix composite, *Acta Metall.* **35** (3), 651–659 (1987).